

# Petrogenetic Evolution of the Eastern Buem Volcanic Rocks, South-Eastern Ghana

Naa A. Agra<sup>1\*</sup>, Daniel Kwayisi<sup>1</sup>, Prince O. Amponsah<sup>3,4</sup>, Samuel B. Dampare<sup>2</sup>, Daniel Asiedu<sup>1</sup>, Prosper M. Nude<sup>1</sup>

<sup>1</sup>University of Ghana, School of Physical and Mathematical Sciences, Department of Earth Science, P.O. Box LG 58, Legon-Accra, Ghana

<sup>2</sup>University of Ghana, School of Nuclear and Allied Sciences, P.O. Box LG 80, Legon-Accra, Ghana

<sup>3</sup>Université de Toulouse, CNRS, Géosciences Environnement Toulouse, Institut de Recherche pour le Développement, Observatoire Midi-Pyrénées, 14 Av. Edouard Belin, F-31400 Toulouse, France

<sup>4</sup>Azumah Resources Ghana limited, PMB CT452, Cantonments, Accra

\*Corresponding author: ntaki@ug.edu.gh

## ABSTRACT

Petrography, major, trace element and Rare Earth Element (REE) data are presented for volcanic rocks from the Eastern Buem Structural Unit (BSU) in south-eastern Ghana to constrain their petrogenesis and tectonic setting. The volcanic rocks are generally aphanitic, ophitic and massive, although some varieties exhibit weak foliation. They are primarily composed of plagioclase and pyroxene. These primary minerals have either partially or wholly altered to chlorite, epidote, sericite and opaque minerals. The basalts have low TiO<sub>2</sub> (0.56–1.19wt. %) content with fairly low magnesium numbers ranging from 38 to 55. They display flat to slightly depleted REE patterns and are mostly more enriched than chondrite. On the primitive mantle (PM) normalised spider diagram, they are variably enriched in Light Rare Earth Elements (LREE) and incompatible elements relative to normal mid-ocean ridge basalt (N-MORB), with similar Large-ion Lithophile Element (LILE) and High Field Strength Element (HFSE) patterns as enriched mid-ocean ridge basalt (E-MORB) but 10 fold more enriched than primitive mantle (PM). They show minor negative and positive Sr, positive Cs, Ba, Ta, La and Ce anomalies and minor negative Rb, Th, Zr and Ti anomalies. The basalts plot within the MORB mantle array on the Th/Yb versus the Nb/Yb diagram and have low Th/Nb ratios (0.07–0.09) which indicate their derivation from asthenospheric sources with minimal or no contamination from crustal or subducted components. They show affinity to Enriched MORB on multi-trace element normalised diagrams. The E-MORB affinity of the basalts is also confirmed on Th–Hf–Nb, Y–La–Nb and V–Ti tectonic discrimination diagrams. These volcanic rocks may have erupted during rifting along the marginal basin of the WAC prior to peak collision during the Pan-African Orogeny.

**Keywords:** Basalt, Buem Structural Unit, Geodynamic evolution, Pan-African Orogeny, Petrogenesis

## Introduction

The 600 Ma Pan African Dahomeyide orogenic belt, which occurs on the eastern margin of the West African Craton (WAC), crops out as the Dahomeyan, Togo and Buem Structural Units in SE Ghana. Rocks in this region are broadly composed of metamorphosed sedimentary packages, para- and ortho-gneisses,

intrusive and volcanic materials which evolved during the Pan African event (Jones, 1990). During the last few years, rocks in this area have been subjected to various age dating geochemical and structural studies. Attoh and Nude (2008) worked on the tectonic significance of carbonatites and ultrahigh-pressure rocks in the suture

zone while Attoh *et al.* (2007) worked on the ages of the carbonatites and alkaline rocks in the suture zone. Others such as Grant (1969); Saunders (1970); Jones (1990); Affaton *et al.* (1997; 1980); Duclaux *et al.*, (2006) and several others have worked on the various rock types, their stratigraphy, and their ages, to understand the Pan-African orogeny.

Of interest to this work are the volcanic packages found within the Buem Structural Unit (BSU). The source component of the BSU volcanics and its geodynamic setting has been an issue of ongoing debate. Two contrasting views have been proposed on the source of the BSU volcanic rocks. According to Jones (1990), the volcanic rocks have characteristics of a consanguineous alkaline lava series in which felsic rocks have evolved by fractional crystallization which formed in a continental rift zone. Affaton *et al.* (1997), on the other hand, proposed that the volcanic mafic lavas were derived from tholeiitic magmas similar to E-MORB, which originated from the partial melting of the lithospheric mantle with a possible asthenospheric contribution. However, Nude *et al.* (2015) described the Buem volcanic rocks as representing mantle derived magmas with both alkaline and subalkaline signatures that may be related to a rifting event and eventual emplacement at the eastern passive margin of the WAC. Work on the Buem volcanic rocks in Ghana (Jones, 1990; Nude *et al.*, 2015) has been mainly on the volcanic rocks within the western BSU. Therefore, in order to have an all-inclusive view and to better characterize the source of the volcanic suites and their relationship to the Pan African event, the petrographic and geochemical characteristics of volcanic rocks of the eastern BSU have been analysed to find out how they compare to the volcanic rocks of the western BSU.

This research seeks to determine the mantle source from which the primary magma of the rocks was generated, magma type, percentage partial melting, depth of magma

generation and contamination, and to establish the relationship between volcanic emplacement and the Pan African Orogeny. The results have been discussed and compared to previous studies done in areas where the BSU outcrops.

### **Regional Geological setting**

The BSU occupies an irregular wide strip of about 15 km which trends NNE-SSW from SE Ghana to the Republic of Benin (Fig. 1). It is divided into the western unit which comprises nappe outliers of the Volta basin and the eastern unit which borders the Togo Structural Unit (Blay, 1991).

In general, BSU is composed of; a) clastic sediments, b) limestone and jasperoids, c) serpentinites d) volcanic rocks and e) intrusive rocks (Fig.2; Agyei Duodu *et al.*, 2009). The clastic rocks comprise sandstones, fine-grained quartzites, siltstones and red shales. They form the uppermost and lowermost parts of the succession. The jasperoids consist of a series of bedded, normally massive and sometimes brecciated red cherts. Some, however, may have formed by metasomatic alteration of the clastic sediments, limestone and volcanic rocks (Junner, 1940; Jones, 1990). Serpentinites are schistose in nature and rich in chromite. Volcanic rocks in the area consist predominantly of basalts, basaltic-andesite, trachytes and phonolite (Nude *et al.*, 2015). Pillow lavas have been recorded in a few places (Junner, 1936). The intrusives are mostly gabbros which are associated with the volcanic rocks (Kwayisi, 2014) and jaspers, and often intrude the shale (Taki, 2014). The BSU is normally unmetamorphosed or locally slightly metamorphosed up to prehnite-pumpellyite facies (Affaton *et al.*, 1997), and has experienced some deformation inferred from the presence of folds, joints and thrust faults within the rocks. The Buem is faulted by the North and South Nkonya fault systems.

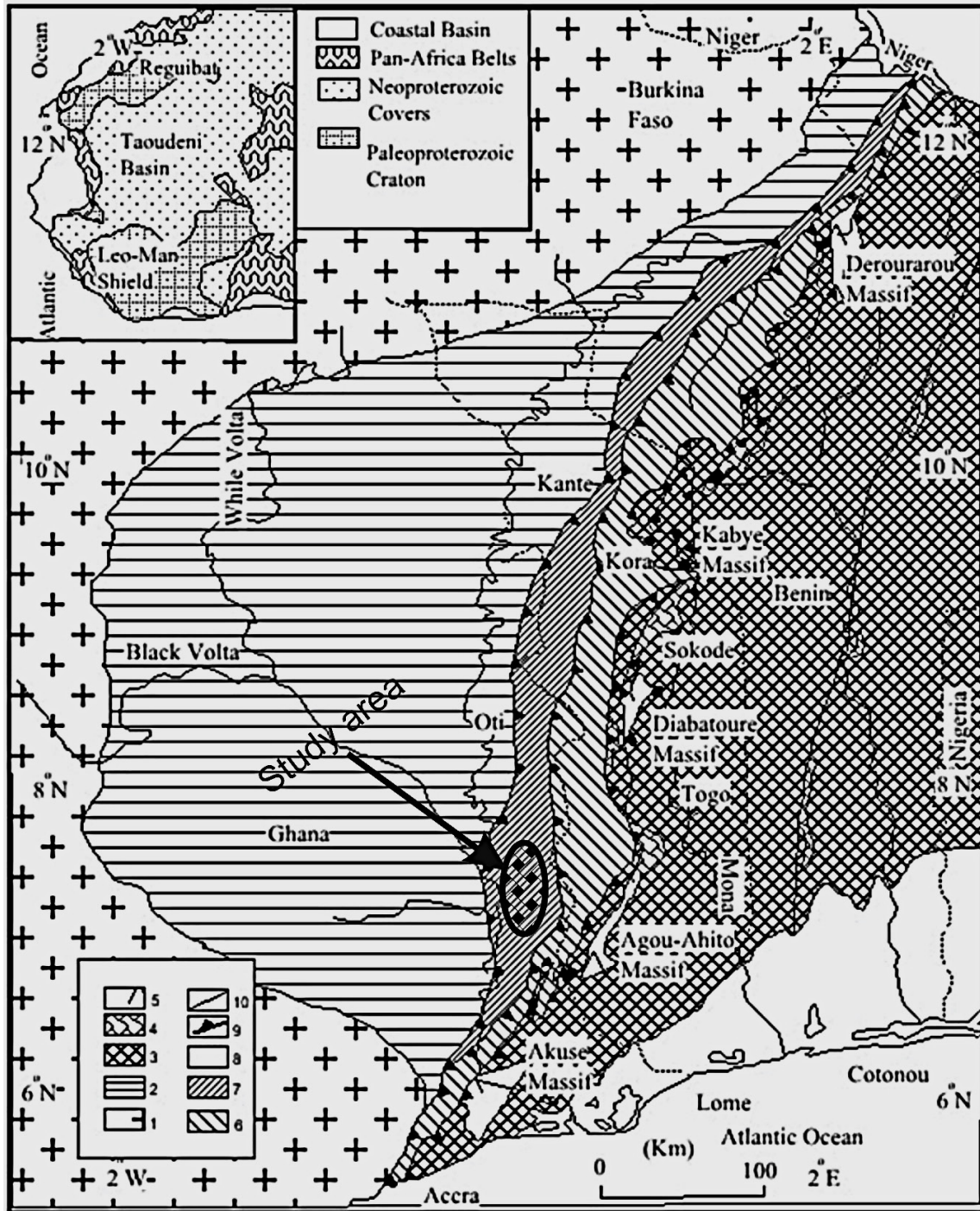


Fig. 1: Dahomeyide orogen showing the major tectonic units (Modified from Affaton *et al.*, 1997). 1 = Eburnean basement complex (WAC); 2 = Neoproterozoic to Paleozoic cover (Volta Basin); 3 = internal and external gneiss-migmatite units; 4 = kyanite bearing micaceous quartzites; 5 = basic and ultrabasic massifs of the suture zone; 6 = Atacora or Akwapim structural unit; 7 = Buem structural unit; 8 = Meso-Cenozoic cover of the Gulf of Guinea Basin; 9 = thrust contact; 10 = Kandi fault mylonitic zone

Folds observed have a general dip to the east, although some of the shales and sandstones dip to the west (Jones, 1990). BSU is considered a tectonic and metamorphic

lateral equivalent of the middle part of the Voltaian supergroup that has been dated 620–640 Ma (Grant, 1969; Affaton et al., 1980).

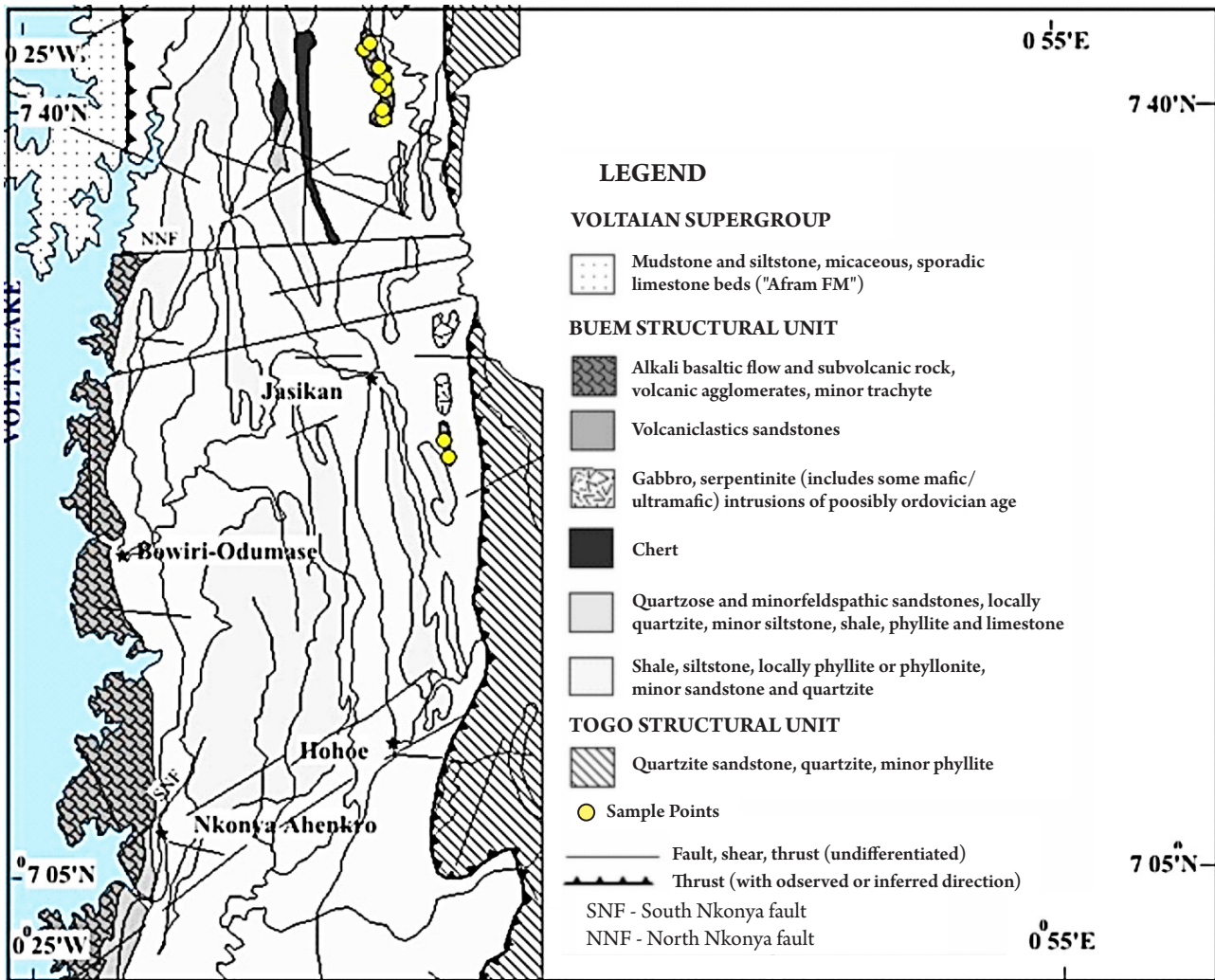


Fig. 2: Geological map of the Buem Structural Unit with yellow circles showing the sampling points (Modified from Agyei Duodu et al., 2009)

## Materials and Methods

Mineralogical and textural relationships of the rock samples were investigated using the Leica DM 750 petrographic microscope at the Department of Earth Science, University of Ghana, Ghana. Whole rock, trace element and REE composition of the samples were analyzed using the Inductively Coupled Plasma Mass-Spectroscopy (ICP-MS) and Inductively Coupled Plasma-Atomic Emission Spectroscopy (ICP-AES) at the ALS Chemex Laboratory in Vancouver, Canada. The major elements were determined using the x-ray fluorescence method on pressed powder pellets. Results obtained were corrected for spectral inter-element interferences and precision was better than 2%.

## Petrography and whole rock geochemistry

### *Lithological and petrographic description*

Most of the volcanic rocks were sampled along rivers and on small hills. The volcanic rocks are greenish or dark grey, fine-grained, dense, and mostly massive except for a few localized areas where they exhibit weak foliation and shear features (Figs. 3A and B). Microscopically, the volcanic rocks are ophitic (Fig. 3C) with few broken crystals and composed primarily of plagioclase and pyroxenes which have undergone various degrees of alteration into sericite, chlorite, epidote and opaque minerals. In some volcanic rocks, euhedral to subhedral plagioclase laths of various sizes, rarely twinned and randomly oriented, occur (Fig. 3D). Quartz- carbonate veinlets cut the volcanic rocks either concordantly or discordantly.

### *Whole rock geochemistry*

The bulk rock major, trace, rare earth element concentrations of the rocks are presented in Table 1 below. The volcanic rocks are characterised by variable major oxide contents.  $\text{SiO}_2$  content varies from 48.88 wt.% to 50.64 wt.%,  $\text{TiO}_2$  from 0.56 wt. % to 1.19 wt.%,  $\text{Al}_2\text{O}_3$  from 13.07 wt.% to 15.31 wt.% and  $\text{Fe}_2\text{O}_3$  content from 6.76 wt.% to 10.40 wt.%, whereas the MgO content ranges from 5.35 wt.% to 10.70 wt.%, CaO from 8.80 wt.% to 13.38 wt.%,  $\text{Na}_2\text{O}$  from 0.42 to 4.04 wt.% and  $\text{K}_2\text{O}$  from 0.02 to 0.54 wt.%.

The magnesium numbers ( $\text{Mg}^\#$ ) of the volcanic rocks are low, spanning a range of 38-55, which shows that the rocks are moderately fractionated. The volcanic rocks have Cr, Ni, Co and V, ranging from 390 to 830 ppm, 113 to 428 ppm, 26 to 50 ppm and 103 to 303 ppm respectively. On the Nb/Y versus Zr/TiO<sub>2</sub> (Fig. 4A) and SiO<sub>2</sub> versus K<sub>2</sub>O (Fig. 4B) diagrams the volcanic rocks plot as sub-alkaline and low K tholeiitic basalts, respectively.

All the volcanic rock samples analyzed are more enriched relative to chondrite except one sample which exhibits a depleted LREE and a flat HREE pattern similar to N-MORB (Fig. 5A). They have  $(\text{La}/\text{Sm})\text{N} = 0.46 - 1.27$  and  $(\text{La}/\text{Yb})\text{N} = 0.36 - 1.38$  with total REE abundance ( $\Sigma \text{REE}$ ) ranging from 20.02 to 53.03 ppm.

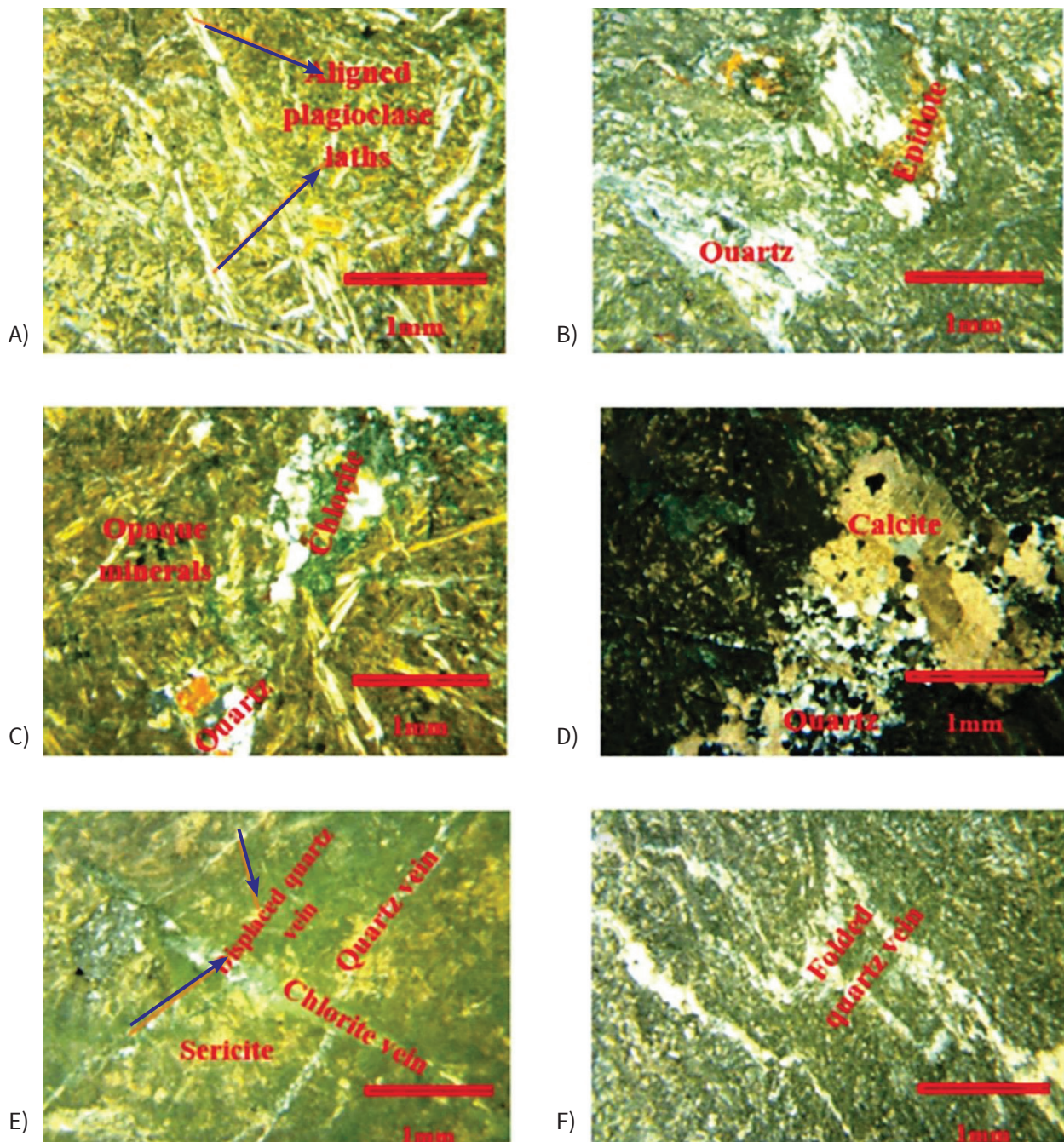


Fig. 3: A) Basalts with stretched and aligned plagioclase laths B) basalt showing epidote and quartz veins occurring together C) photomicrograph showing chlorite and quartz veins occurring together in basalt D) quartz and carbonate veins occurring together in basalt E) photomicrograph of basalt showing quartz vein cut by a chlorite vein F) basalt showing folded quartz vein.

On a primitive mantle (Sun and McDonough, 1989) normalized spider diagram, the volcanic rocks exhibit a flat pattern, but are more enriched in both LILE and HFSE than primitive mantle. They exhibit enrichment in Cs, Sr, Ba, Ta, La, Ce and Hf, and depletion in Sr, Rb,

Th, K, Zr and Ti, with a relatively flat HFSE pattern (Fig. 5B). On the other hand, their multi-element pattern is similar to that of E-MORB, yet they are more enriched than N-MORB and depleted relative to OIB.

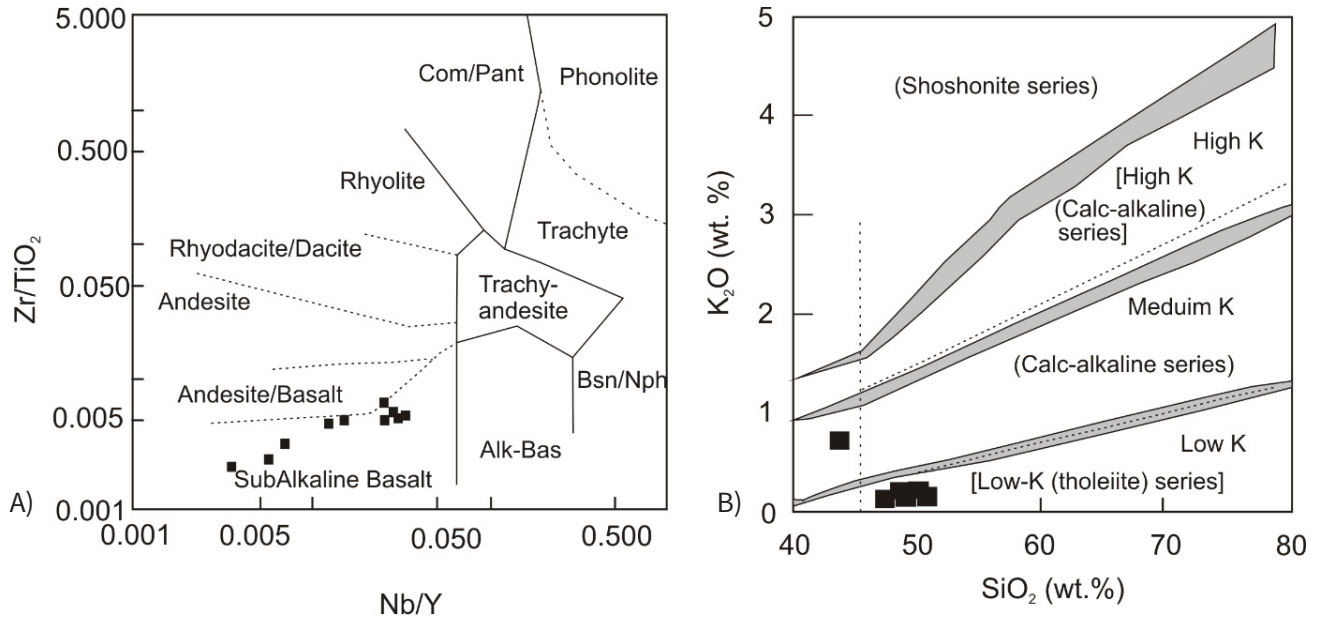


Fig. 4: A) Nb/Y versus Zr/TiO<sub>2</sub> plot of Winchester and Floyd (1977), B) K<sub>2</sub>O versus SiO<sub>2</sub> binary diagram by Le Maitre (1989), for the nine (9) sampled basalts

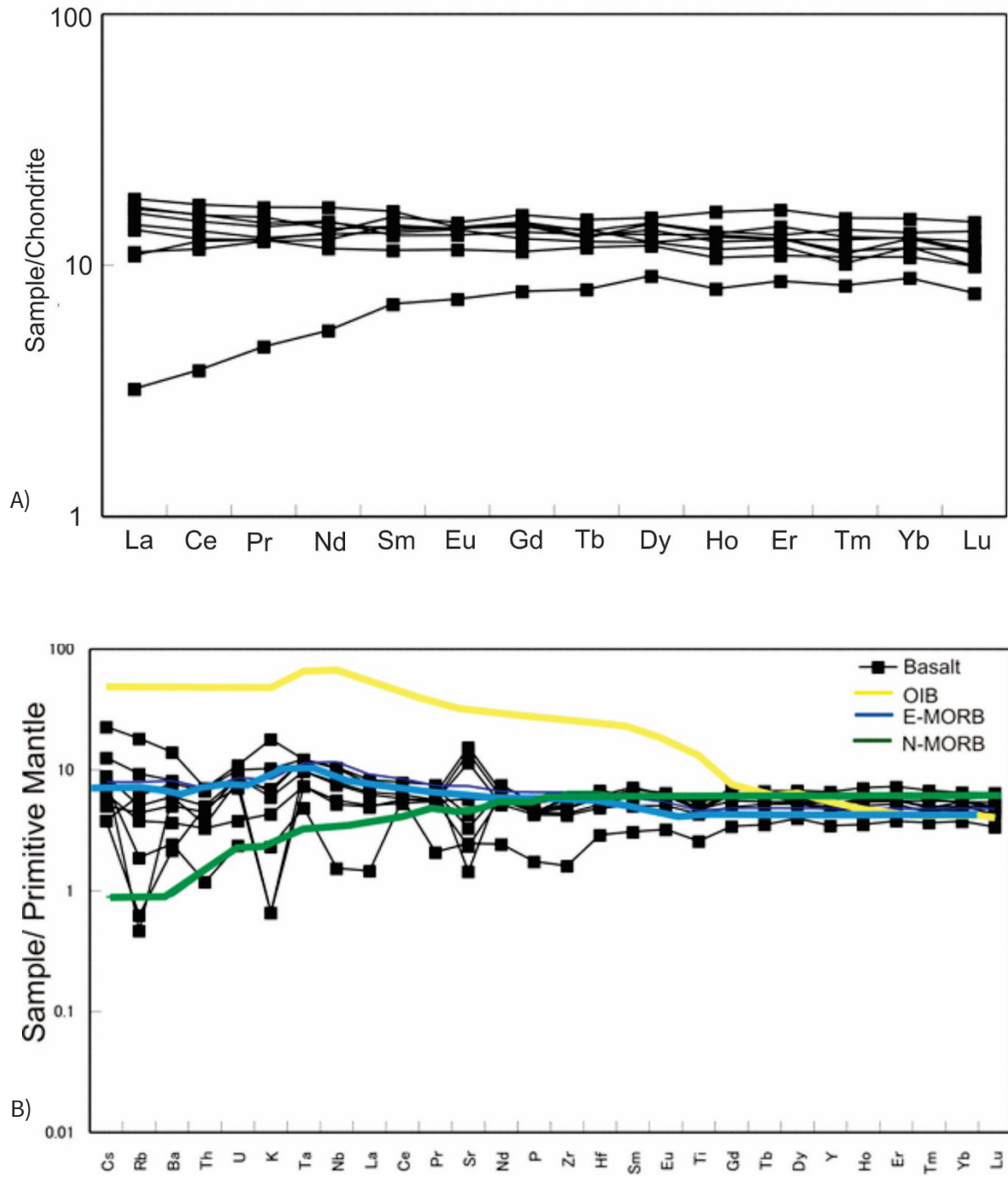


Fig. 5: A) Chondrite normalized REE plot, B) Primitive mantle normalized multi-element plot, for the nine (9) sampled basalts

**Table 1: Major and trace element compositions of the basalts**

wt.%	NT-TT-006A	NT-TT-006B	NT-TT-006B1	NT-TT-007A	NT-TT-007B	NT-TT-008	NT-TT-009A	NT-TT-009B	NT-TT-011
SiO <sub>2</sub>	49.19	50.58	49.16	48.48	46.88	48.91	50.64	47.31	47.60
TiO <sub>2</sub>	0.94	1.02	1.01	1.19	1.16	1.16	1.18	0.56	1.07
Al <sub>2</sub> O <sub>3</sub>	13.07	14.62	14.68	15.31	14.97	14.87	15.23	14.30	14.10
Fe <sub>2</sub> O <sub>3</sub>	9.06	6.76	6.80	7.83	9.99	8.56	8.66	8.64	10.40
MnO	0.17	0.14	0.15	0.14	0.17	0.15	0.13	0.15	0.18
MgO	8.54	6.35	6.16	6.37	9.66	7.45	5.35	10.70	6.73
CaO	13.38	11.44	12.05	10.32	8.80	10.51	11.69	11.56	12.38
Na <sub>2</sub> O	0.42	2.59	2.74	3.38	2.29	3.05	4.04	1.69	1.75
K <sub>2</sub> O	0.02	0.18	0.20	0.31	0.54	0.21	0.02	0.07	0.13
P <sub>2</sub> O <sub>5</sub>	0.09	0.10	0.10	0.10	0.12	0.10	0.10	0.04	0.10
LOI	4.98	5.67	6.63	5.94	4.86	4.86	2.84	4.34	5.11
Total	99.96	99.56	99.80	99.46	99.51	99.91	99.97	99.47	99.62
Mg #	55.80	48.50	48.40	44.90	49.20	46.50	38.20	55.30	39.30
Na <sub>2</sub> O+K <sub>2</sub> O	1.89	0.44	2.77	3.69	2.83	3.26	4.06	1.76	1.88
ppm									
Cr	760.00	430.00	550.00	490.00	460.00	390.00	470.00	830.00	460.00
Ni	428.00	123.00	110.00	151.00	133.00	129.00	113.00	230.00	137.00
Co	26.00	39.00	45.00	50.00	43.00	48.00	48.00	49.00	44.00
V	103.00	254.00	263.00	299.00	303.00	280.00	286.00	238.00	294.00
Cu	3.00	60.00	74.00	74.00	70.00	78.00	59.00	100.00	68.00
Zn	29.00	63.00	74.00	80.00	72.00	93.00	96.00	60.00	76.00
Cs	0.03	0.04	0.07	0.10	0.18	0.03	0.07	0.06	0.05
Rb	0.40	2.80	3.20	5.90	11.60	3.90	0.30	1.20	2.40
Ba	15.00	35.30	42.00	57.50	98.30	54.10	42.00	17.10	25.50
Th	0.42	0.38	0.43	0.59	0.60	0.57	0.30	0.10	0.28
U	0.15	0.18	0.18	0.21	0.23	0.17	0.17	0.05	0.08
Nb	5.40	5.60	6.20	7.40	7.50	7.30	3.70	1.10	4.00
Ta	0.40	0.40	0.50	0.50	0.50	0.50	0.30	0.20	0.30
K	166.00	1494.00	1660.00	2573.00	4483.00	1743.00	166.00	581.00	1079.00
La	4.30	4.50	5.00	5.20	5.70	5.30	3.40	1.00	3.50
Ce	10.30	11.10	12.10	12.90	14.10	12.80	10.10	3.10	9.40
Pr	1.54	1.57	1.74	1.80	2.08	1.90	1.54	0.58	1.52
Sr	241.00	294.00	327.00	70.00	30.30	89.90	49.40	52.10	121.50
P	405.90	419.00	423.40	427.70	506.30	427.70	449.60	165.90	423.40
Nd	7.00	8.00	8.90	9.00	10.20	8.40	8.10	3.30	7.60

Table 1 Continues

wt.%	NT-TT-006A	NT-TT-006B	NT-TT-006B1	NT-TT-007A	NT-TT-007B	NT-TT-008	NT-TT-009A	NT-TT-009B	NT-TT-011
Sm	2.24	2.63	2.70	2.57	3.20	2.78	3.04	1.37	2.82
Zr	47.00	67.00	49.00	64.00	64.00	59.00	55.00	18.00	54.00
Hf	1.50	2.10	1.60	1.90	1.90	1.80	1.80	0.90	1.80
Eu	0.85	1.02	1.04	0.97	1.04	1.03	1.09	0.54	1.03
Ti	5635.00	6115.00	6055.00	7134.00	6954.00	6954.00	7074.00	3357.00	6415.00
Gd	2.94	3.31	3.68	3.52	3.85	3.82	4.11	2.04	3.73
Tb	0.56	0.59	0.66	0.63	0.65	0.62	0.72	0.38	0.61
Dy	3.86	3.98	3.98	4.28	4.75	4.46	4.98	2.93	4.71
Y	21.20	22.10	24.10	23.30	26.10	24.20	30.00	15.80	26.10
Ho	0.77	0.83	0.93	0.95	0.98	0.89	1.17	0.58	0.96
Er	2.30	2.50	2.68	2.68	2.77	2.65	3.50	1.82	3.00
Tm	0.35	0.33	0.37	0.36	0.45	0.41	0.50	0.27	0.42
Yb	2.26	2.47	2.45	2.67	2.82	2.70	3.21	1.86	2.68
Lu	0.32	0.32	0.37	0.36	0.44	0.37	0.48	0.25	0.40

## Discussion

From the information presented so far, the magma source, magma type, percentage partial melting, tectonic setting and others will be determined and discussed.

## Alteration

The occurrence of secondary minerals such as chlorite, epidote and carbonates-quartz veins shows that the rocks are altered. LOI values of the volcanic rocks are moderate to high (2.84-6.63 wt. %), and this, coupled with scattered to positive correlation between SiO<sub>2</sub> and LOI (Fig. 6A), also suggests alteration and SiO<sub>2</sub> remobilisation in the volcanic rocks. Hence, before attempting petrogenetic and tectonic setting interpretation, it is important to evaluate the effect of alteration on the samples. The lack of correlation between LOI and Nb/La and Th/La (not shown) suggests that the primary Th-Nb-LREE concentrations in the rocks have not been disturbed much by hydrothermal alteration or metamorphism. Also, according to Gaffney *et al.* (2004) and Shervais *et al.* (2006), K<sub>2</sub>O/P<sub>2</sub>O<sub>5</sub> > 1 indicates that samples have not undergone significant post-cooling alteration, which would mobilize K relative to P. Notwithstanding 2 samples with K<sub>2</sub>O/P<sub>2</sub>O<sub>5</sub> < 1, the K<sub>2</sub>O/P<sub>2</sub>O<sub>5</sub> ratios

for the volcanic rocks range from 1.54 to 4.66, which are mostly greater than 1. This also suggests minimal element mobility or alteration of the rocks. In addition, linear relations observed between Zr and most of the elements, especially REE, the transition elements and HFSE in the volcanic rocks, connote relative immobility of these elements. Therefore, although these rocks are altered, some of the elements' (REE, HFS and Transition elements) concentrations have been preserved in the rock. Thus, for petrogenetic and tectonic setting interpretations, we focused mainly on the immobile elements.

## Petrogenesis

### Magma differentiation/ Fractional crystallization

A decrease in MgO, CaO, Al<sub>2</sub>O<sub>3</sub> and FeO<sub>t</sub> and an increasing SiO<sub>2</sub> observed on variation diagrams could suggest the fractional crystallisation of olivine, clinopyroxene and plagioclase in basalts during the early stages of magma evolution. However, clinopyroxene and plagioclase were observed in thin sections. The MgO content of the volcanic rocks is below 14 wt. % and coupled with the low magnesium numbers, suggests that

the rocks may have experienced some fractionation. On the AFM diagram (Fig. 6B), the samples plot away from MgO but towards FeO, which also suggests that the rocks have experienced some fractionation.

It is sometimes difficult to differentiate between the effects of fractional crystallization and/or partial melting on the compositions of primary magmas. However, compatible–incompatible element plots such as Ni and Th versus SiO<sub>2</sub> may provide a clue to the type of process taking place. Fractionation of ferromagnesian minerals such as olivine and clinopyroxene usually decreases the concentrations of compatible elements (e.g., Ni and Cr) and increases the concentrations of incompatible elements such as Th, La and Nd in the liquid (Dampare et

al., 2008). In the plots of Ni and Th versus SiO<sub>2</sub> (Fig. 7A & B), the volcanic rocks show a decrease in compatible and an increase in incompatible element concentrations with increasing SiO<sub>2</sub> content. It can be inferred from these plots that the volcanic rocks evolved mostly by fractional crystallization, but the effect of partial melting in the evolution of these rocks cannot be ruled out due to the high Th content as well as the dispersed trend observed from the Th versus SiO<sub>2</sub> diagram.

The fractional crystallisation trend observed in the volcanic rocks is further supported by the (La/Lu) chond versus Mg# diagram of Shervais et al. (2006). An increase in La/Lu with decreasing Mg# suggests assimilation of crustal component with fractional crystallisation

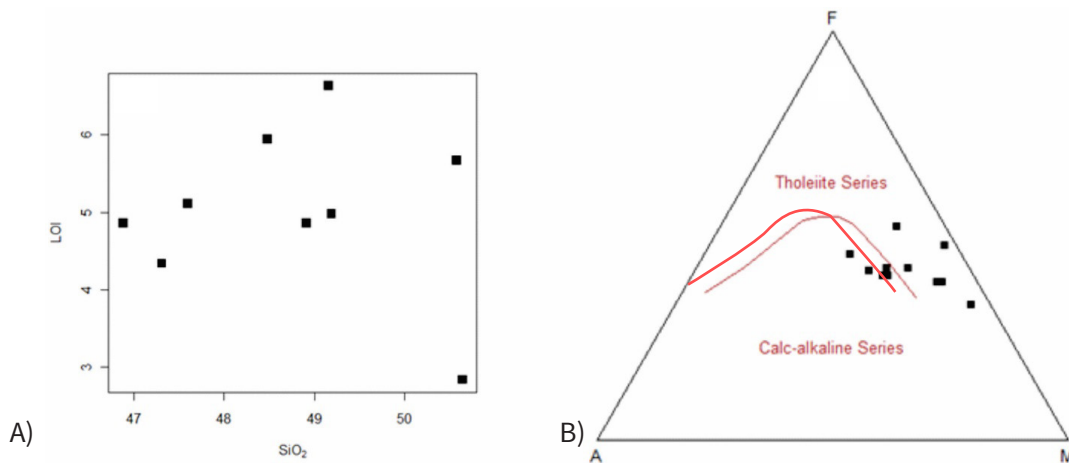


Fig. 6: A) LOI versus SiO<sub>2</sub> plot, B) AFM diagram by Irvine and Baragar (1971) plotted for the nine (9) basalts

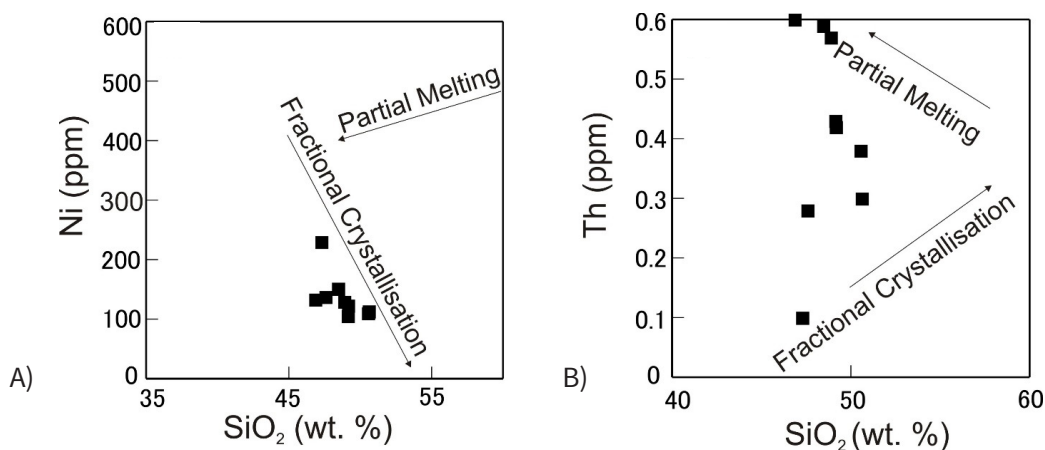


Fig. 7: A) SiO<sub>2</sub> versus Ni, B) SiO<sub>2</sub> versus Th plots for the nine (9) sampled basalts

(Shervais *et al.*, 2006). The low La/Lu content (Fig. 8) of the volcanic rocks thus suggests minimal or no assimilation of crustal component following fractional crystallisation. The flat REE pattern of the volcanic rocks and their La/Sm (= 0.46 – 1.27) and La/Yb (0.36 – 1.38) ratios suggest that the rocks have experienced minimal fractionation.

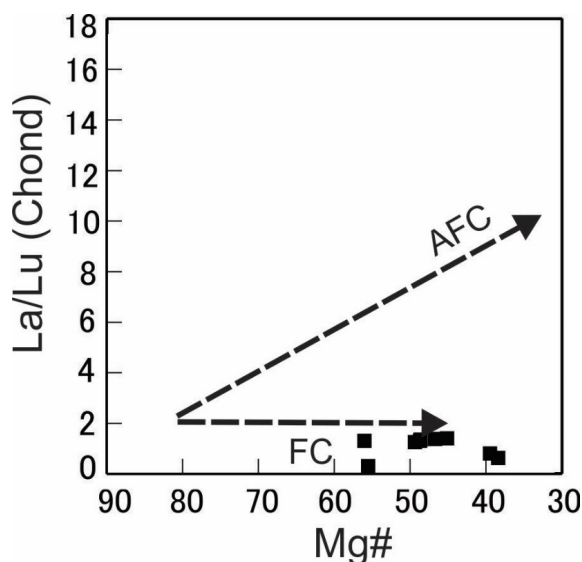


Fig. 8: (La/Lu) chond versus Mg# plot for the rocks (Shervais *et al.*, 2006).

### Modelling of magma source, enrichment and contamination

Earlier workers have shown that the elemental ratios such as Th/Yb, Nb/Yb and Ta/Yb emphasize source variations and crustal assimilation as they are mostly independent of fractional crystallization and/or partial melting (Dampare *et al.*, 2008). Basaltic magmas which have been derived from the mantle asthenosphere (Depleted MORB Mantle), the plume asthenosphere or the mantle lithosphere enriched by a small degree of melt from the asthenosphere, often fall within or close to a diagonal mantle array defined by constant Th/Nb and Th/Ta values. Th, rather than Nb, Ta or Yb, is usually entrained in subduction zone components. Source components that have been metasomatised by subduction processes

will be enriched in Th relative to Nb or Ta, thereby resulting in higher Th/Yb ratios than Nb/Yb or Ta/Yb. Crustal contamination may also increase Th/Yb values with respect to Nb/Yb or Ta/Yb values, as crustal rocks also contain relatively higher concentrations of Th than Nb and Ta. The volcanic rocks were plotted on the Th/Yb versus Nb/Yb diagram of Pearce (1983), Pearce and Peate (1995) and Pearce (2014; Fig. 9), where they plotted within the mantle array and span the area between N-MORB and E-MORB. This suggests that the volcanic rocks have not experienced any form of contamination, either from the crust or by subducted component.

Johnson and Plank (1999) interpreted the fluid-immobile element Th (e.g., the Th/Nb value) as a proxy for melted and recycled sediment. The Th/Nb ratios for the volcanic rocks span a range of 0.07 to 0.09, which is very low. This also confirms that the volcanic rocks were generated from a mantle source which has not experienced any contribution from melted and recycled sediments, as shown by the Th/Yb and Nb/Yb diagram (Fig. 9). The mantle source of the rocks was determined in the Th–Nb–Ce systematics of oceanic basalts proposed by Saunders *et al.* (1988). According to the authors, the Th–Nb–Ce systematics of oceanic basalts could be visualized in terms of mixing between a depleted MORB source mantle (DMM: relatively high Ce/Nb), a recycled residual slab component processed through the subduction zone (RSC: low Ce/Nb), and a recycled subduction component complementary to RSC (SDC: high Th/Nb).

The rock samples were plotted in a Ce/Nb versus Th/Nb diagram (Fig. 10), following the approach of Kerrich *et al.* (1999). All the samples plotted in the field of E-MORB. This may suggest that the rocks were generated solely from an enriched source in the mantle rather than through enrichment by crustal or subducted material.

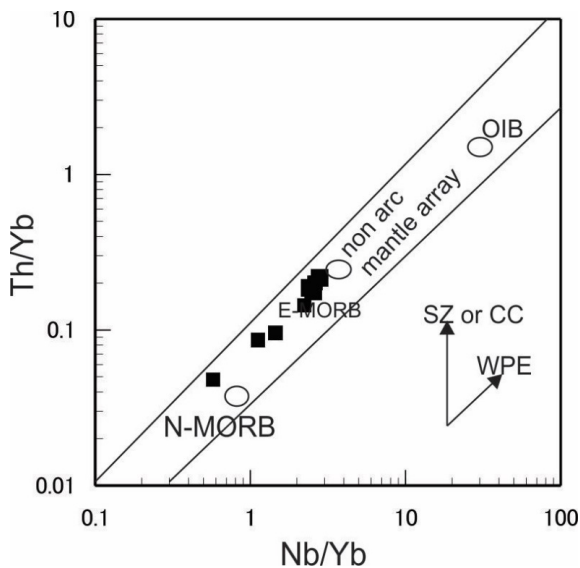


Fig. 9: Th/Yb versus Nb/Yb diagram (after Pearce, 1983; Pearce and Peate, 1995, Pearce, 2014) of the nine (9) sampled rocks illustrating the input of Th from either subduction-zone enrichment or crustal contamination (CC). Samples with very little subducted slab influence lie within or very close to the ‘mantle’ array defined by the N-MORB array whereas samples influenced by subducted slab flux are displaced from the ‘mantle’ array to higher Th at a given Nb content than do the former. WPE: within-plate enrichment; SZ: subduction zone flux. N-MORB, E-MORB, and OIB from Sun and McDonough (1989).

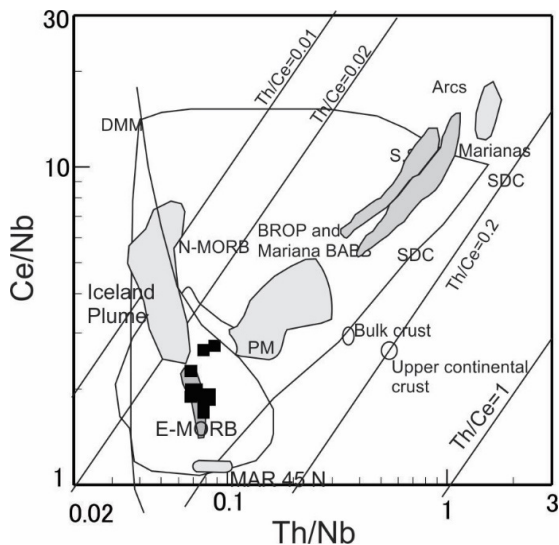


Fig. 10: Plot of Th/Nb vs. Ce/Nb (after Saunders *et al.*, 1988) for the nine (9) sampled basalts. DMM: depleted MORB mantle; E-MORB: enriched mid-ocean ridge basalt; N-MORB: normal mid-ocean ridge basalt; OIB: oceanic island basalt; MAR45°N: Mid Atlantic Ridge 45°N; PM: primitive mantle; RSC: recycled residual slab components; SDC: recycled subduction derived component. Lines indicate mixing trajectories between components. Also shown are the compositions of the bulk crust and upper continental crust, as well as the fields of Ontong Java Ocean Plateau (OJOP), Broken Ridge Ocean Plateau (BROP), Back Arc Basin Basalts (BABB) and Iceland Plume basalts. Diagram was adopted from Dampare *et al.* (2008) and references therein.

**Evaluation of the source characteristics of the basalts and REE modeling of partial melting.**

The composition of the mantle source, residual mineralogies and degree of partial melting that produced the parental magmas of basalts can be determined using REE abundances and ratios (Aldanmaz *et al.*, 2000). The non-modal batch partial melting equations of Shaw (1970) and the REE partition coefficients of McKenzie and O’Nions (1991) were used to model the degree of partial melting for the volcanic rocks. Usually, modelling should involve only the least evolved samples; thus, samples with relatively higher Mg numbers ( $Mg \geq 55$ ), elevated Ni and Cr abundances ( $>100$  ppm) and low REE abundances should be used. Although the Mg numbers of the volcanic rocks are relatively low, they were used for the modelling since they have Ni and Cr concentrations ( $>100$  ppm) and low REE abundances. Following Aldanmaz *et al.* (2000), two different reference compositions were used to define the likely mantle array: (1) depleted MORB mantle (DMM) which was assumed to represent the convecting asthenospheric mantle with the composition of the hypothetical depleted MORB source proposed by McKenzie and O’Nions (1991); and (2) Primitive Mantle (PM; Sun and McDonough, 1989) which represents the initial mantle composition prior to MORB formation and depletion.

The contents of the highly incompatible element La and the less incompatible element Sm in basalts can be used to constrain the bulk source compositions, since their concentrations are not influenced much by the variations in either spinel-bearing or garnet-bearing source mineralogies (Aldanmaz *et al.*, 2000; Dampare *et al.*, 2008). From the samples plotted on Fig. 11A, it can be observed that most of the rocks have La concentrations and La/Sm ratios greater than those that could be

generated by direct melting of DMM, even when the degree of partial melting is very small (0.1%). It can therefore be inferred that one-stage melting of DMM (or PM) cannot produce magma with incompatible element content similar to those of the basalts. A mantle source that has been enriched in LREE relative to DMM composition is required to produce the basaltic magma since the rocks plot closer to E-MORB (Sun and McDonough, 1989).

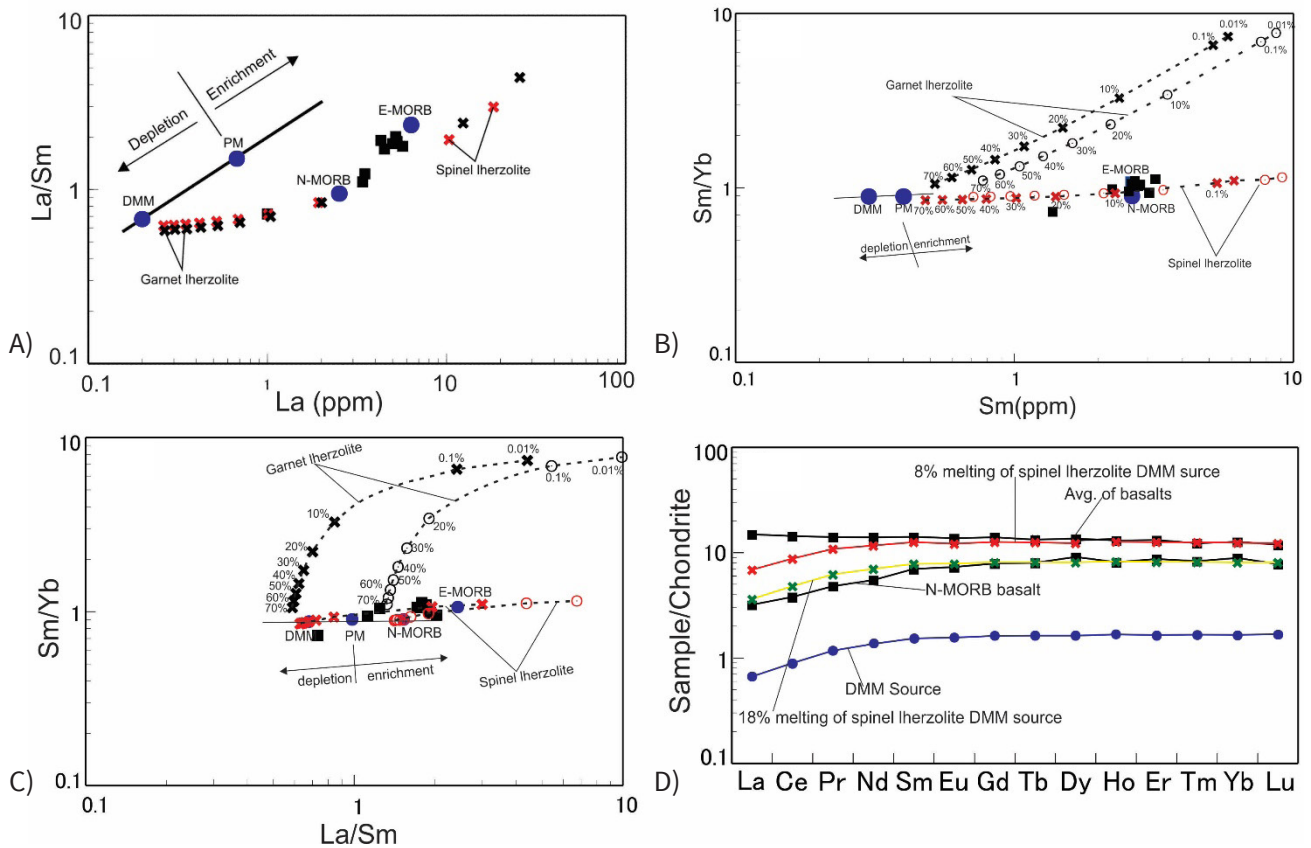


Fig. 11: A) La vs. La/Sm, B) Sm/Yb vs. Sm and C) Sm/Yb vs. La/Sm, D) REE Spectrum modelling for the nine (9) Eastern Buem basalts. Melting curves (lines) for spinel–lherzolite (ol53 + opx27 + cpx17 + sp3) and garnet–peridotite (ol60 + opx20 + cpx10 + gt10) sources with both DMM and PM compositions were drawn following the approach of Aldanmaz *et al.* (2000). Open circles and crosses on the melting curves correspond to degrees of partial melting for a given mantle source. The heavy line represents the mantle array defined by depleted MORB mantle (DMM; McKenzie and O’Nions, 1991) and primitive mantle (PM, Sun and McDonough, 1989) compositions. The N-MORB and E-MORB compositions (Sun and McDonough (1989) have also been shown.

The Sm/Yb ratios can be used to determine the source mineralogy of basaltic rocks, because Yb is compatible with garnet but not with clinopyroxene or spinel. Partial melting of a spinel lherzolite mantle source does not change the Sm/Yb value because both Sm and Yb have similar partition coefficients, whereas it may decrease La/Sm values and Sm contents of the melts as melting progresses. Melts derived from spinel lherzolite sources would be expected to produce melting trends that are sub-parallel to and nearly coincident with a mantle array defined by depleted to enriched source compositions (Fig. 11B and C). However, melts generated by small to moderate degrees of garnet lherzolite melting with residual garnet would have Sm/Yb values significantly higher than Sm/Yb values in the mantle source(s). This will produce melting trends of garnet lherzolite that is displaced from the DMM-PM “mantle” array to higher Sm/Yb. (Aldanmaz *et al.*, 2000; Zhao *et al.*, 2007; Dampare *et al.*, 2008). It is observed from Figs. 11B and C that most of the volcanic rocks plot close to the spinel lherzolite melting curve between 1-10% partial melting, except one N-MORB-like sample that plots close to the 20% partial melting curve. This suggests that the enriched rocks were generated by about 1-10% partial melting of a spinel lherzolite source that is more enriched than DMM and PM since they plot close to E-MORB while the N-MORB-like sample was generated by about 20 % melting of a spinel lherzolite from a DMM source. The high LILE content of the basalts relative to N-MORB and PM is also confirmed by their incompatible multi-element diagram (Fig. 6). The degree of partial melting was also constrained by modeling a spinel lherzolite source for the entire REE spectrum (Fig. 11D). From Fig. 11D it can be confirmed that the average basalt composition of the enriched rocks can be generated by about 8% partial melting of a depleted spinel lherzolite source that has been enriched, since the volcanic rocks are relatively enriched in LREE (La, Ce, Pr, Nd and Sm) compared to DMM. The enrichment processes are mostly considered to be due to either small volume melt fractions or subduction-related fluids (McKenzie, 1989; Anderson, 1994), and are therefore restricted to the non-convecting (lithospheric) mantle. The N-MORB-

like sample on the other hand was generated from about 18% partial melting of a spinel lherzolite from the DMM source.

From the REE model therefore it can be inferred that the volcanic rocks may have been generated by a two stage partial melting, the first by the melting of an enriched source to produce the enriched basalts. Continuous melting of the previously enriched source that has been depleted by earlier melt extraction generated the magma that formed the depleted N-MORB-like sample. This mechanism could be attributed to a multi-stage emplacement of basaltic magma within the eastern BSU as a result of the occurrence of volcanic rocks with N-MORB and E-MORB signatures within the BSU. The results compare with recent work by Nude *et al.* (2015), in which the authors inferred multi-stage emplacement for the western Buem volcanic rocks due to their distinct petrography and geochemical characteristics. Hence, taken together, volcanism in the BSU can be considered as episodic with source fractionation at different depths and emplacement at different periods.

According to Winter (2001), depth of origin of plagioclase lherzolite, spinel lherzolite and garnet lherzolite is from 0-40 km, 40-80 km and greater than 80 km respectively. Since it has been inferred that the rocks were generated by partial melting of a spinel lherzolite source, their approximate depth of generation will be from about 40-80 km according to the literature.

### **Tectonic Setting**

Immobile element proxy discrimination diagrams have been employed to complement the patterns observed on incompatible multi-element diagrams for identifying the tectonic setting of the rocks. The volcanic rocks from the Eastern BSU show enriched MORB characteristics as they plot in the field of E-MORB, within plate tholeiitic basalts on the Th-Hf-Nb tectonic discrimination by Wood (1990; Fig. 12A), except for one sample that plots in the field of N-MORB. The E-MORB affinity of the basalts is further confirmed on the Y/La/Nb discrimination diagram of Cabanis and Lecolle (1989; Fig. 12B), where

the basalts plot in the field of anorogenic E-MORB. Shervais (1982) proposed the V–Ti discrimination diagram, on which lava compositions shift from low V/Ti in MORB lavas through intermediate V/Ti in island arc tholeiites (IAT) to high V/Ti in boninites. On this diagram, volcanic arc basalts have Ti/V ratios ranging between 10 and 20, MORB has ratios between 20 and 50, and oceanic island arcs and alkaline basalts between 50 and 100. Most of the volcanic rocks plot in the field of Ocean Floor basalts on this diagram (Fig. 12C), which supports their MORB-like affinity.

In Fig. 5B the volcanic rocks define a similar trend as E-MORB, with slight depletion in LILE but flat HREE pattern. This, therefore, suggests that the volcanic rocks originated from an enriched MORB source within the

mantle. Rocks with MORB-like affinity can occur in different tectonic settings, but will have distinct geochemical signatures with which they can be identified. However, since the volcanic rocks do not show geochemical signatures similar to arcs materials, it can be inferred that the volcanic rocks were emplaced in a rifted environment prior to the Pan-African peak collisional event. Nude *et al.* (2015) observed similar geochemical characteristics for the volcanic rocks of western BSU and suggested that the rocks may be related to rifting of a strongly attenuated continental crust that may have preceded the onset of the Pan-African collision. Hence, a similar tectonic setting can be inferred for the eastern Buem volcanic rocks. Considering all these, the volcanic rocks of the BSU may be related to a rifting event and eventual emplacement at the eastern margin of the WAC.

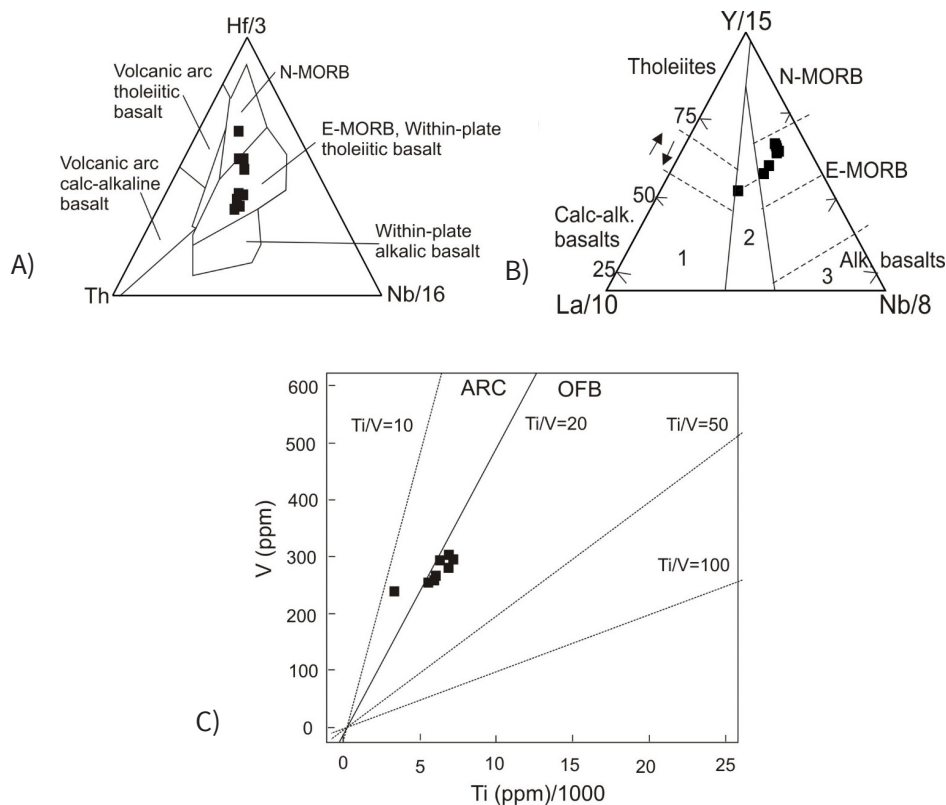


Fig. 12: A) Th–Hf–Nb triangular discrimination diagram of Wood (1990), B) Y/La/Nb discrimination diagram (after Cabanis and Lecolle, 1989); 1: orogenic domains; 2: late- to post-orogenic continental domains; 3: anorogenic domains, C) V versus Ti diagram of Shervais 1982, plotted for the nine (9) Eastern Buem basalts.

## Conclusion

The volcanic rocks are sub alkaline and appear to have originated from a low-K tholeiitic magma series by low degree partial melting of an enriched mantle source with possible asthenospheric contribution.

Geochemical characteristics suggest that these volcanic rocks are mantle derived magmas that have an affinity to E-MORB with minimal or no contamination from subducted sediment or crustal component. Major and trace element variation patterns suggest that the rocks were not derived from primary magma but have evolved through fractional crystallisation of clinopyroxene and plagioclase. From trace element modelling, the enriched basalts were generated from about 8-9% melting of a spinel lherzolite from a DMM source that has been enriched, while the typical N-MORB-like sample was generated from about 18% partial melting of spinel lherzolite from a DMM source. The approximate depth of generation of the volcanic rocks is between 40 and 80 km. The eastern Buem volcanic rocks show similar petrographic and geochemical characteristics as the western Buem volcanic rocks, Hence, the two may have formed in the same tectonic environment. Thus, rifting that may have occurred prior to the Pan-African collision and emplacement at the eastern margin of the WAC.

## Acknowledgements

We are grateful to the Department of Earth Science, University of Ghana (capacity building project) for funding this research. We would also like to thank the entire teaching and non-teaching staff of the Department of Earth Science (University of Ghana) for their support. We are also grateful to the chief, the Bani family and the people of Jasikan for their hospitality during our stay in the town.

## References

- Affaton, P., Aguirre, L. & Menot, R.P. (1997). Thermal and geodynamic setting of the Buem volcanic rocks near Tiélé, Northwest Benin, West Africa. *Precambrian Research*, 82, 191–209 and all references therein.
- Affaton, P., Sougy, J. & Trompette, R. (1980). The tectono-stratigraphic relationships between the Upper Precambrian and Lower Paleozoic Volta Basin and the Pan-African Dahomeyide Orogenic Belt (West Africa). *American Journal of Science*, 280, 224-248.
- Agyei Duodu, J., Loh, G.K., Boamah, K.O., Baba, M., Hirdes, W., Toloczyki, M., & Davis, D.W. (2009). *Geological Map of Ghana 1:1 000 000*. Geological Survey Department of Ghana (GSD).
- Aldanmaz, E., Pearce, J.A., Thirlwall, M.F. & Mitchell, J.G. (2000). Petrogenetic evolution of late Cenozoic, post-collision volcanism in western Anatolia, Turkey. *Journal of Volcanology and Geothermal Research*, 102, 67–95.
- Anderson, D.L. (1994). The sublithospheric mantle as the source of continental flood basalts; the case against the continental lithosphere and plume head reservoirs. *Earth Planet Science Letter*, 123, 269-280.
- Attoh K., Corfu F. & Nude P.M. (2007). U-Pb zircon age of deformed carbonatite and alkaline rocks in the Pan-African Dahomeyide suture zone, West Africa. *Precambrian Research*, 155, 251-260.
- Attoh K. & Nude P.M. (2008). Tectonic significance of carbonatite and ultrahigh-pressure rocks in the Pan-African Dahomeyide suture zone, southeastern Ghana. *Geological Society of London, Special Publication*, 297, 217–231.
- Blay, P.K. (1991). The Geology of ¼ Field Sheet No. 184, Hohoe N.E.
- Cabanis, B. & Lecolle, M. (1989). Le diagramme La/10-Y/15-Nb/8: un outil pour la discrimination des series volcaniques et la mise en evidence des processus de mdlange et/ou de contamination

- crustale. C. R. Academy Science Paris 309, 2023-2029.
- Dampare, S.B., Shibata, T., Asiedu, D.K., Osae, S. & Banoeng-Yakubo, B. (2008). Geochemistry of Paleoproterozoic metavolcanic rocks from the southern Ashanti volcanic belt, Ghana: Petrogenetic and tectonic setting implications. *Precambrian Research*, 162, 403–423.
- Duclaux G., Ménot R.P., Guillot S., Agbossoumondé Y. & Hilairet N. (2006). The mafic layered complex of the Kabyé massif (north Togo and north Benin): Evidence of a Pan-African granulitic continental arc root. *Precambrian Research*, 151, 101-118.
- Gaffney, A.M., Nelson, B.K. & Blichert-Toft, J. (2004). Geochemical Constraints on the Role of Oceanic Lithosphere in Intra-Volcano Heterogeneity at West Maui, Hawaii. *Journal of Petrology*, 45 (8), 1663–1687.
- Grant, N.K. (1969). The Late Precambrian to early Palaeozoic Pan-African Orogeny in Ghana, “Togo, Dahomey and Nigeria. *Bulletin of Geological Society of America*, 80, 45-55.
- Irvine, T.N. & Baragar, W.R.A. (1971). A guide to the chemical classification of the common volcanic rocks. *Canadian Journal of Earth Science*, 8, 523-548.
- Johnson, M.C. & Plank, T. (1999). Dehydration and melting experiments constrain the fate of subducted sediments. *Geochemical Geophysics and Geosystems*, 1. doi: 10.1029/1999GC000014.
- Jones, W.B. (1990). The Buem volcanic and associated sedimentary rocks, Ghana: a field and geochemical investigation. *Journal of African Earth Science*, 11, 373-383.
- Junner, N.R. (1936). *Volta River District and Togoland under British Mandate*. Gold Coast Geological Survey Annual Report, 1935-36, 10-16.
- Junner, N.R. (1940). Geology of the Gold Coast and Western Togoland. *Gold Coast Geological Survey Bulletin*, 11.
- Kerrich, R., Polat, A., Wyman, D. & Hollings, P. (1999). Trace element systematics of Mg-to Fe-tholeiite basalt suites of the Superior Province: implication for Archaean mantle reservoirs and greenstone belt genesis. *Lithos* 46, 163–187.
- Kwayisi, D. (2014). Petrology and geochemistry of western Buem volcanic rocks, southeastern Ghana: geodynamic setting implication (unpublished master’s thesis). University of Ghana, Legon. 140 pp.
- Le Maitre, R.W. (1989). *A classification of igneous rocks and glossary of terms*. In: Le Maitre, R.W. (Ed.), Recommendations of the International Union of Geological Sciences, Subcommittee on Systematics of Igneous Rocks. Blackwell Science Publication, 193 pp.
- McKenzie, D.P. (1989). Some remarks on the movement of small volume melt fractions in the mantle. *Earth Planet Science, Letter* 95, 53-72.
- McKenzie, D. & O’Nions, R.K. (1991). Partial melt distribution from inversion of rare earth element concentrations. *Journal of Petrology*, 32, 1021–1091.
- Nude, P.M., Kwayisi, D., Taki, N. A., Kutu, J. M., Anani, C. Y., Banoeng-Yakubo, B. & Asiedu, D. K. (2015). Chemical evidence for multi-stage emplacement of western Buem volcanic rocks in the Dahomeyide orogenic belt, Southeastern Ghana, West Africa. *Journal of African Earth Science*, 112, 314-327.
- Pearce, J.A. (1983). *Role of the sub-continental lithosphere in magma genesis at active continental margins*. In: Hawkesworth, C.J., Norry, M.J. (Eds.), *Continental Basalts and Mantle Xenoliths*. Shiva Publication Limited, Cheshire, UK, 230–249.
- Pearce, J.A. (2014). Immobile Element Fingerprinting of Ophiolites. *Elements*, 10, 101–108.
- Pearce, J.A. & Peate, D.W. (1995). Tectonic implications of the composition of volcanic arc magmas. *Annual Review Earth Planet Science*, 23, 251–285.

- Saunders, A.D., Norry, M.J. & Tarney, J. (1988). Origin of MORB and chemically depleted mantle reservoirs: trace element constraints. *Journal of Petrology*. (Special Lithosphere Issue), 415–445.
- Saunders, S.R. (1970). Early Paleozoic Orogeny in Ghana: Foreland Stratigraphy and Structure. *Geological Society of America Bulletin*, 81, 233-240.
- Shaw, D.M. (1970). Trace element fractionation during anatexis. *Geochim. Cosmochim. Acta*. 34, 237–243.
- Shervais, J.W. (1982). Ti–V plots and the petrogenesis of modern and ophiolitic lavas. *Earth Planet Science Express*, 59, 101–118.
- Shervais, J.W., Vetter, S.K. & Hanan, B.B. (2006). Layered mafic sill complex beneath the eastern Snake River Plain: Evidence from cyclic geochemical variations in basalt. *Geology*, 34 (5), 365–368.
- Sun, S. & McDonough, W.F. (1989). Chemical and isotopic systematic of oceanic basalts: implications for mantle composition and processes. In: Saunders, A.D., Norry, M.J. (Eds.), *Magmatism in the Ocean Basins. Geological Society Special Publication*, 42, 313-345.
- Taki, N. A. (2014). Petrogenetic evolution of the eastern Buem mafic suite, southeastern Ghana (unpublished master's thesis). University of Ghana, Legon. 96 pp.
- Winchester, J.A. & Floyd, P.A. (1977). Geochemical discrimination of different magma series and their differentiation products using immobile elements. *Chemical Geology*, 20, 325–343.
- Winter, J. (2001). *Introduction to igneous and metamorphic petrology*. Prentice Hall Upper Saddle River, New Jersey 07458, 796 pages.
- Wood, D.A. (1990). The application of a Th–Hf–Ta diagram to problems of tectonomagmatic classification and to establishing the nature of crustal contamination of basaltic lavas of the British Tertiary volcanic province. *Earth Planet Science Letter*, 50, 11–30.
- Zhao, J-H, Zhou & M-F. (2007). Geochemistry of Neoproterozoic mafic intrusions in the Panzihua district (Sichuan Province, SW China): Implications for subduction-related metasomatism in the upper mantle. *Precambrian Research*, 152, 27–47.